TOPICAL REVIEW— Topological insulator

Molecular-beam epitaxy of topological insulator Bi_2Se_3 (111) and (221) thin films*

Xie Mao-Hai(谢茂海)†, Guo Xin(郭 欣), Xu Zhong-Jie(徐忠杰), and Ho Wing-Kin(何永健)

Physics Department, The University of Hong Kong, Pokfulam Road, Hong Kong, China

(Received 2 April 2013)

This paper presents an overview of the growth of Bi_2Se_3, a prototypical three-dimensional topological insulator, by molecular-beam epitaxy on various substrates. Comparison is made between the growth of Bi_2Se_3 (111) on van der Waals (vdW) and non-vdW substrates, with attention paid to twin suppression and strain. Growth along the [221] direction of Bi_2Se_3 on InP (001) and GaAs (001) substrates is also discussed.

Keywords: topological insulator, molecular-beam epitaxy, Bi_2Se_3, twin domain, strain

PACS: 81.15.–z, 81.10.–h, 68.55.–a, 68.37.–d **DOI:** 10.1088/1674-1056/22/6/068101

1. Introduction

Characterization of the quantum properties of topological insulators (TIs) requires high-quality samples. Early experiments on the surface electronic structures of three-dimensional (3D) TIs were made on bulk crystals prepared by thermal cooling of stoichiometric melts, for example.[1–4] Although such bulk samples exhibited good structural and electronic qualities, they were not very suitable for transport studies. Consequently, more recent efforts have been increasingly directed toward growing TI thin-film samples by epitaxial methods, such as molecular-beam epitaxy (MBE).[5–20] This approach is particularly fruitful because of the ultrahigh vacuum aspect of MBE, which makes characterization of the sample's surface viable during or immediately after growth, eliminating potential complications due to surface contamination from the ambient environment.[2,21] Moreover, thin films are particularly suitable for making gated device structures, which are essential for chemical potential tuning in transport experiments.[10,11,15,16,22]

In this paper, we present an overview of some of the recent findings and results of the MBE growth of Bi_2Se_3 compound, a prototypical 3D topological insulator.[1,23] We pay particular attention to the general growth properties and elaborate on twin domain suppression and strain relaxation in epitaxial Bi_2Se_3 on different substrates. Growth of Bi_2Se_3 along both the [111] and [221] directions will be discussed.

2. General growth properties

Bi_2Se_3 was among the first few 3D topological insulators discovered by theory and experiment (others include Bi_2Te_3 and Sb_2Te_3).[1,23] Bi_2Se_3 is particularly attractive because it has a relatively large energy bandgap in its bulk (~ 0.3 eV), holding the promise of high-temperature applications. Crystalline Bi_2Se_3 has a rhombohedral structure with the space group $R\bar{3}m$. It can also be described in terms of a hexagonal primitive cell containing three quintuple layers (QLs) of alternating selenium (Se) and bismuth (Bi) atoms stacked in the sequence of –[ABCAB]–[CABCA]–[BCABC]– along the trigonal (c-) axis. Here –[$\cdots$]– denotes one Bi_2Se_3 QL composed of two Bi atomic layers sandwiched between three Se layers. The atoms within each QL unit are chemically bonded, whereas the bonds between adjacent QLs are the weak van der Waals (vdW) force. The "gap" between the vdW-force bonded atomic planes is a natural cleavage plane, which is readily obtained by cleavage of a bulk crystal or by growth of an epitaxial film. Such a plane, i.e., Bi_2Se_3 (111), is the only surface that has been extensively studied so far by surface techniques such as angle-resolved photoemission spectroscopy (ARPES) and scanning tunneling microscopy and spectroscopy (STM/STS),[1,2,7,8,24].

Bi_2Se_3 (111) has been found to grow readily on many different substrates with wide variations in lattice constants. It reflects the nature of the van der Waals epitaxy (vdWe)[25,26] of the material. The unique layered structure of Bi_2Se_3 in the c-axis direction makes two-dimensional (2D) nucleation and growth of the compound along [111] favorable. Past experiments have unambiguously shown that the growth unit of Bi_2Se_3 is one QL, in which Se and Bi are strongly bonded.[5,6] If one uses a substrate that is inert in terms of chemical interaction with deposited Bi_2Se_3, the heterointerface is governed by vdW bonding and growth follows the familiar vdWe process.

*Project supported by the Research Grant Council (RGC) of Hong Kong Special Administrative Region for its financial support under the General Research Funds (Grant Nos. 706110 and 706111) and the SRFDP and RGCERG Joint Research Scheme sponsored by the RGC of Hong Kong and the Ministry of Education of China (M-HKU709/12).

†Corresponding author. E-mail: mhxie@hku.hk

© 2013 Chinese Physical Society and IOP Publishing Ltd

Also, because of the weak vdW bonding, growth of Bi_2Se_3 is quite tolerant of the choice of substrate. Many substrates that people have used include silicon (Si),[5,6,17,27] GaAs,[9] InP,[17,19,20] CdS,[12,16] graphene,[28] CaF_2,[18] sapphire,[15] $SrTiO_3$,[10] GaN and SiC,[29] to name a few. All of these have resulted in Bi_2Se_3 (111) films. The large variation in lattice misfits between Bi_2Se_3 and these substrates does not appear to be critical, although small lattice misfits do tend to bring about better quality films.[16,19,20,29] The lattice misfit strain may readily be accommodated at the vdW interface without breaking chemical bonds. As will be shown later in this paper, the first QL Bi_2Se_3 deposited on a vdW type of substrate (e.g., Si:H) shows a lattice parameter that is indistinguishable from that of a bulk crystal according to *in situ* reflection high-energy electron diffraction (RHEED) measurements. On a non-vdW type of substrate (such as GaAs), the residual strain in the first QL Bi_2Se_3 appears greater.

Before discussing the growth characteristics of Bi_2Se_3 on different substrates, we first comment on the MBE conditions that are appropriate for Bi_2Se_3 epitaxy. At vacuum levels of 10^{-7} Torr–10^{-10} Torr (1 Torr = 1.33322×10^2 Pa), typical for Bi_2Se_3 MBE, the solid phase of stoichiometric Bi_2Se_3 is in equilibrium with the vapor phases of Bi and Se at relatively low temperatures.[30] Experiments have shown that the optimal temperature for growth is in the range of 150 °C–250 °C. In general, a higher temperature is favored for enhanced surface diffusion and thus smoother surface morphology. But at too high a temperature, condensation is incomplete. As for the flux of Bi and Se sources, according to the phase diagram,[30] one has to choose an Se flux that is in excess of stoichiometry (i.e., a flux ratio Se:Bi $>$ 3:2). On the other hand, because the flux of Se generated from a conventional Knudsen cell is composed mainly of Se tetramers (Se_4), whose decomposition is not very efficient, a much higher Se flux will be needed — usually about 10 times that of Bi, or even more. If one has access to a cracker cell, Se-dimers (Se_2) will be the main constituent in the vapor and a lower ratio between Se and Bi fluxes (e.g., Se:Bi $\sim$ 3:1) can be accepted.[18]

3. Bi_2Se_3 epitaxy on hex-symmetrical substrate surfaces

So far, the majority of epitaxial Bi_2Se_3 films have been grown on substrate surfaces with hexagonal lattice symmetries, such as the (111) surfaces of cubic or rhombohedral crystals or the (0001) surfaces of wurtzite compounds. Such choices of substrates are natural, because the hexagonal lattice symmetry of the Bi_2Se_3 (111) surface is the same. For the various substrates employed, one may make a distinction between those where there are no unsaturated dangling bonds of the surface atoms and are thus of the vdW type, and those with dangling bonds (non-vdW type). Graphene and hydrogen-terminated Si (Si:H) obviously belong to the former category, while clean InP(111)A and sapphire (0001) are of the latter type. It is worth comparing the growth behaviors on these two different categories of substrates. Furthermore, lattice misfits differ for different substrates. Understanding how the misfit strain affects the growth properties of Bi_2Se_3 and how it is relaxed during growth is of both scientific and practical value.

3.1. Bi_2Se_3 deposition on vdW substrates

A number of early MBE Bi_2Se_3 growth experiments were performed using the Si (111) substrate due to the obvious reasons of its wide availability, low cost, and mature processing technology. Silicon, the most important semiconductor, has an in-plane lattice parameter that is not too far from that of Bi_2Se_3 (0.384 nm for Si versus 0.414 nm of Bi_2Se_3). However, clean Si (111) is (7 $\times$ 7) reconstructed with dangling unsaturated bonds. So upon Bi_2Se_3 deposition, Se atoms may react with surface Si, forming $SiSe_2$, for example.[27,31] If this occurs, it will not favor van der Waals epitaxy of Bi_2Se_3. Our experiments have shown that direct deposition of Bi_2Se_3 on clean Si (111)-(7 $\times$ 7) at elevated temperatures does not result in single-crystalline epifilms, which is evidenced by the ring patterns in the RHEED, signaling a polycrystalline film.[29] In order to facilitate a crystalline epifilm growth on Si (111), one thus has to modify the surface prior to Bi_2Se_3 deposition. A number of methods have been developed for Si surface treatment, including dosing the surface with a coverage of Bi for a β-($\sqrt{3}\times\sqrt{3}$) reconstructed surface,[5] depositing a thin InSe buffer,[14] and exposing the surface to a flux of Se for an Se-terminated one[32]. For the latter, one must be careful to choose a suitable temperature so as to avoid $SiSe_2$ formation. In a previous study, we adopted a more parameter-tolerant method: depositing a thin amorphous Bi–Se buffer at a cryostat temperature of $\sim$ 100 K followed by annealing and subsequent deposition at an elevated temperature of 520 K.[6] We found that the method was effective in producing crystalline Bi_2Se_3 films.

A more common and simple approach to passivating the dangling bonds on Si (111) is H-atom termination, which can be achieved simply by dipping the Si wafer into hydrofluoric acid.[33] The surface then becomes (1 $\times$ 1) structured instead of (7 $\times$ 7). Growth of Bi_2Se_3 on such a surface follows the vdWe process.[25,26] Figure 1 presents an STM image of a Bi_2Se_3 sample grown on Si (111):H by direct deposition at 490 K.[29] As is seen, the surface is dominated by triangular mounds with the steps on mounds being a single QL high ($\sim$ 1 nm). Such a morphology is characteristic of Bi_2Se_3 (111) films grown on flat substrate surfaces.[6] The triangular shape of the mounds reflects the three-fold symmetry of the Bi_2Se_3 crystal about the c axis. Kinetically, it is pro-

duced by anisotropic growth rates of two inequivalent sets of steps on the surface that are governed by the bonding characteristics of atoms at these steps.[34]

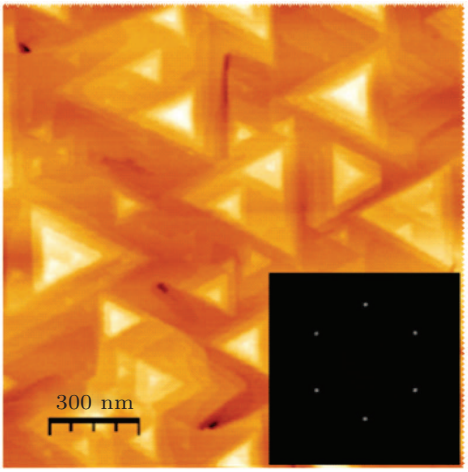


Fig. 1. STM micrograph of a Bi_2Se_3 film grown on an Si (111):H substrate (reprinted from *J. Cryst. Growth* **334**, Z. Y. Wang *et al.*, "Growth characteristics of topological insulator Bi_2Se_3 films on different substrates", pp. 96–102 (2011), with permission from Elsevier).[29] The inset shows the LEED pattern (taken at 40 eV) for such a surface, revealing the six-fold symmetry of the lattice.

In the following, we draw attention to the orientation of the triangular mounds in Fig. 1. Note that they are not aligned, but oppositely oriented. Such oppositely oriented mounds are a common feature in the morphology of epitaxial Bi_2Se_3 on Si:H and other vdW substrates. This reflects the fact that the epifilm contains twin domains. Indeed, the orientation of the triangular mounds signifies the stacking order of atoms in Bi_2Se_3 (Fig. 2). If the film is single-domain with uniform in-plane alignment, the mounds ought to be aligned in one and the same direction. The oppositely oriented mounds seen in Fig. 1 reveal the coexistence of different stacking orders in the sample and thus a twinned film. A twinned film would be globally six-fold symmetrical about the surface normal, which can be verified by low-energy electron diffraction (LEED) measurements. This is shown in the inset of Fig. 1. Twinning of epitaxial Bi_2Se_3 on a flat vdW substrate may be understood from the fact that there is a weak vdW interaction between Bi_2Se_3 and the substrate, and so the *sub*surface layer of atoms in the substrate may not play a role in constraining the lattices of the deposit. If so, i.e., only the top surface layer with the six-fold lattice symmetry guides the epitaxy of Bi_2Se_3, then two equivalent stacking configurations of the Bi_2Se_3, ABCAB and ACBAC, will be equally probable, giving rise to the twinned film (Fig. 2). One may tune the growth parameters to affect the domain size; however, twin defects on flat vdW substrates can hardly be eliminated so long as growth proceeds in the 2D nucleation mode.

In order to suppress twin formation, one may "turn on" the guiding role of the subsurface layer(s) of the substrate by choosing a substrate that strongly interacts with Bi_2Se_3 during deposition, so that the subsurface atoms are influential in determining the epitaxial alignment of the deposit. Alternatively, one may adopt a vicinal substrate on which trains of steps exist. Atoms at step edges have dangling bonds, favoring strong chemical interaction. Step-edge atoms will then affect the epitaxial stacking of Bi_2Se_3, promoting a single, substrate-lattice-aligned domain under the step-flow growth mode. Figure 3 shows an example of a Bi_2Se_3 film grown on vicinal Si (111). Instead of triangular mounds, the surface is composed of terraces and steps. A single domain Bi_2Se_3 film can be inferred from the RHEED pattern shown in the inset of Fig. 3, where the diffraction spots (marked by yellow dots) are seen to be asymmetrically distributed.[29] Twin suppression has brought about improved electronic properties of the material, which are exemplified by reduced background doping and enhanced electron mobility.[6,20]

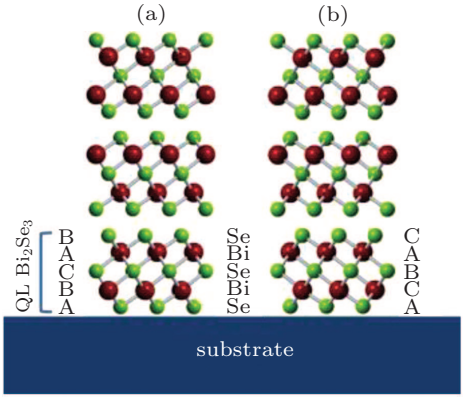


Fig. 2. Stick-and-ball model of a primitive cell of Bi_2Se_3 on a substrate but stacked in different configurations for panels (a) and (b).

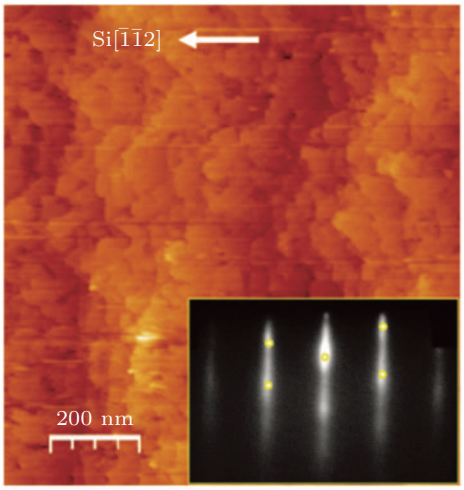


Fig. 3. STM micrograph of a Bi_2Se_3 film grown on a vicinal Si surface (3.5° offcut from (111) toward). Inset: a RHEED pattern taken at the early stage of Bi_2Se_3 deposition (electron energy 10 keV, and incident along Si [$\bar{1}\bar{1}$0]) (reprinted from *J. Cryst. Growth* **334**, Z. Y. Wang *et al.*, "Growth characteristics of topological insulator Bi_2Se_3 films on different substrates," pp. 96–102 (2011), with permission from Elsevier).[29] Note the asymmetric distribution of the spotty diffraction feature signaling a suppression of the twin domain in such a film.

Another interesting aspect of Bi_2Se_3 growth on vdW substrates is the lattice misfit strain. With *in situ* RHEED, we

can monitor in-plane lattice parameter evolution of the deposit in real time. We find that upon Bi_2Se_3 deposition, a new set of diffraction patterns emerge in the background of a pattern from the substrate surface. An example is given in the inset of Fig. 4, obtained from growth on a flat Si (111):H surface. Measuring the spacing D between the two integer streaks and comparing it to D_{Si}, the value of the Si substrate, we derive the in-plane lattice parameter of the deposit at various stages of growth. As it happens, at the very early stage of deposition when the diffraction streaks corresponding to the Bi_2Se_3 deposit have just emerged, the measured in-plane lattice constant is found to be indistinguishable from that of a bulk Bi_2Se_3 crystal (green line and open circles in Fig. 4). Therefore, the nucleation islands of Bi_2Se_3 on Si:H (and on other vdW substrates) appear to be strain-relieved. Such strain-free QL-high Bi_2Se_3 islands on the vdW substrates would be consistent with the weak interaction between Bi_2Se_3 and the substrate at their interfaces, and so Bi_2Se_3 epifilm can hardly be strained by the lattice of the substrate. However, to our surprise, we find that the lattice constant of the growing Bi_2Se_3 continues to evolve with deposition coverage and reaches a maximum of approximately 0.418 nm at $\sim$ 1 QL before gradually coming to match the bulk value of 0.414 nm. This is shown in Fig. 4. So there is $\sim$ 1% lattice stretch over a bulk Bi_2Se_3 crystal at $\leq$ 1 QL coverage. Despite being small, such a stretched in-plane lattice constant is obvious and repeatable. We do not know the reason behind this observation. One might attribute it to the equilibrium lattice constant of an ultrathin Bi_2Se_3 layer that is inherently different from the bulk crystal.[35] Nevertheless, our preliminary calculations have provided no strong evidence of such. Further studies are needed to elucidate the origin of such an observation.

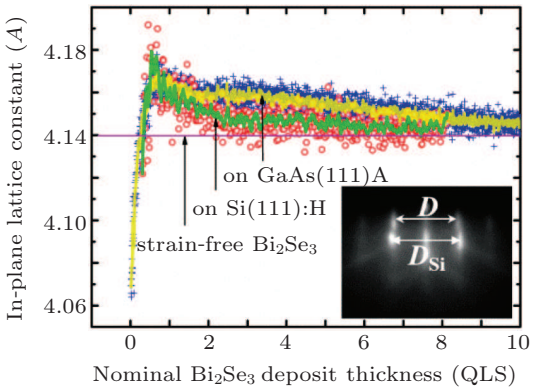


Fig. 4. The in-plane lattice constant measured by RHEED as Bi_2Se_3 deposition proceeded. The red open circles are for growth on Si (111):H, while the blue crosses are for growth on GaAs(111)A. The superimposed green and yellow lines represent data following five-adjacent-point-averaging for each case. The horizontal pink line indicates the lattice constant of a strain-free Bi_2Se_3. The inset shows a RHEED pattern taken at the sub-QL deposition stage of Bi_2Se_3 on Si (111):H, where two sets of diffraction patterns coexist, one from the substrate and the other from epitaxial Bi_2Se_3. The in-plane lattice constants shown in the main figure are derived from the inter-streak spacing D, as defined in the figure.

3.2. Bi_2Se_3 deposition on non-vdW substrates

We now turn to the growth properties of Bi_2Se_3 on non-vdW substrates. We carried out the growth experiments on sapphire (0001), InP (111), GaAs (111), and SiC (0001) of this category. While InP's lattice constant closely matches that of Bi_2Se_3, the others have relatively large lattice misfits, so there is again a strain-relaxation issue. On such substrates, atoms have dangling bonds, which may lead to strong chemical interaction between the substrate and Bi_2Se_3 deposit. Taking InP(111)A (the indium-terminated face) as an example, each indium (In) atom on the surface has an "empty" hybridized bond, which would readily interact with the outermost Se atom that has a lone pair orbital. This makes the epitaxy of Bi_2Se_3 on InP resemble that of covalent semiconductors. The strong chemical interaction between In and Se is verified by first principles calculations.[20] Such an interaction at the heterointerface would make the lattice of ultrathin Bi_2Se_3 layers strain to fit the substrate's lattice. Although this is hardly seen in Bi_2Se_3-on-InP due to its small lattice mismatch, on other substrates of similar character such as GaAs(111)A, we expect the strain to be observable in the films. Note, however, that as Bi_2Se_3 grows in a unit of one QL, which has a thickness of $\sim$ 1 nm, the strain energy could already be too high to sustain a fully strained Bi_2Se_3 QL on substrates with relatively large lattice misfits.[36,37] Therefore, in general, the films are partially strained. This appears to be the case indeed, as shown in Fig. 4 (crosses and yellow line) recorded during Bi_2Se_3 deposition on GaAs(111)A. Note the seemingly smaller lattice constants of the initially nucleated Bi_2Se_3 islands on GaAs (a substrate having an in-plane lattice parameter of $\sim$ 4 Å, 1 Å = 0.1 nm) (yellow line and blue crosses). This indicates that the Bi_2Se_3 nucleated on GaAs (111) is indeed partially strained. Similar to growth on vdW substrates, the lattice parameter also evolves with deposition coverage, showing a lattice stretch at about 1 QL.

Another interesting observation of Bi_2Se_3 growth on InP(111)A and GaAs(111)A is the diminished twin defects in the epifilms. Figure 5 shows an example of a surface of Bi_2Se_3 grown on InP(111)A. The surface is again composed of triangular mounds. These mounds are, however, uniformly oriented toward one and the same direction, suggesting single-domain films according to the previous discussions. The LEED measurements show diffraction patterns of three-fold symmetry (Fig. 5 inset), confirming the single domain of the epifilm.[20]

In passing, we wish to comment on the step structures on the mounds. Often, the mounds are spirals with winding steps at the sides, which are caused by preferential growth at dislocations.[38] Recently, a new mechanism has been proposed wherein a spiral mound forms via growth-front pinning followed by upward climbing of a portion of the pinned growth front over a step.[39] An examination of the

mounds in Fig. 5, however, reveals that they have a wedding-cake structure. Wedding-cake-shaped mounds were previously reported in some other epitaxial systems such as metals and semiconductors,[40,41] and were attributed to an Ehrlich–Schwoebel barrier.[42,43] This observation of the wedding-cake mounds in Bi_2Se_3 calls for a study of the surface kinetics of the system in such a direction.

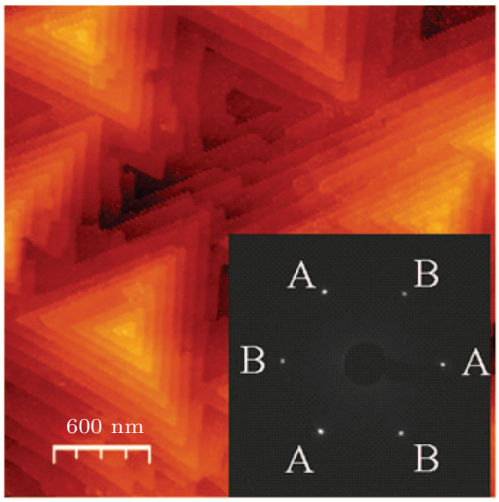


Fig. 5. STM micrograph of a Bi_2Se_3 film grown on InP(111)A. Note the unidirectional mounds, signaling a single-domain epifilm, which is further confirmed by the three-fold LEED pattern (taken at an energy of 40 eV) shown in the inset (note the two sets of diffraction spots, marked by "A" and "B", showing different intensities).

Returning to twin suppression in epitaxial Bi_2Se_3 on InP and GaAs substrates, one might think it is related to a strong chemical interaction between the substrate and epitaxial Bi_2Se_3, through which the subsurface layer(s) of the substrate affect the stacking of the atoms of epitaxial Bi_2Se_3. However, total energy calculations comparing the two stacking configurations of one QL Bi_2Se_3 on a six-bilayer InP "substrate," $[ABCABC]_{InP}$–$[abcab]_{Bi_2Se_3}$ versus $[ABCABC]_{InP}$–$[acbac]_{Bi_2Se_3}$, suggest that the two stackings are more or less degenerate, with the rotated stacking being slightly more favorable, by ~ 8 meV/(1×1) cell.[20] Experimentally, we observed an aligned epitaxial relation, i.e., $Bi_2Se_3[111]$|| InP[111] and $Bi_2Se_3[\bar{1}\bar{1}2]$ || InP$[\bar{1}\bar{1}2]$, which is at odds with the calculation. Thus we believe that the twin domain suppression in Bi_2Se_3 on InP and GaAs is again explained by the epifilm's lattice being constrained by the steps of the substrate. In fact, subsequent experiments on carefully treated substrates with large terraces, where Bi_2Se_3 growth is proceeded by island nucleation, resulted in epifilms that were indeed twinned. On the other hand, step-flow growth on vicinal InP substrates consistently produced single-domain films.[20]

In some previous studies, the phosphorus-terminated InP(111)B surface was adopted as the substrate for Bi_2Se_3 epitaxy.[19] Phosphorus atoms on InP(111)B have lone electron pairs, which makes Bi_2Se_3 growth on top of it vdWe-like. We have examined the formation energy of Bi_2Se_3QL on InP(111)B and found an energy cost of 0.489 eV per (1×1) cell over that on InP(111)A.[20] So despite the fact that Bi_2Se_3 does grow on InP(111)B, it is less favorable than growth on the In-terminated InP(111)A surface. Another promising substrate is CdS, which also has a small lattice misfit with Bi_2Se_3. Surface atoms of CdS have similar bonding characteristics to InP, so similar growth behaviors may be expected.

Finally, a point worthy of attention is the terrace-and-step morphology of epitaxial Bi_2Se_3 on vicinal substrates (such as that in Fig. 3). This morphology is typical for step-flow growth of covalent semiconductors, and the epifilm and substrate are thus c axis parallel (see Fig. 6(a)), i.e., $Bi_2Se_3[111]$ || InP[111], for example. Such a "coherent" epitaxial relation is, however, not one of the characteristics of van der Waals epitaxy in a strict sense. For the latter, one would expect a Bi_2Se_3 film to "float" on the stepped substrate surface, and its c axis would be parallel to the surface normal (refer to Fig. 6(b)). The [111] direction of an InP substrate and the Bi_2Se_3 epifilm would then differ by an angle θ equal to the offcut angle of the substrate. The fact that this is not the case may again reflect a strong chemical interaction of atoms at steps that prevents such strict vdW processes.

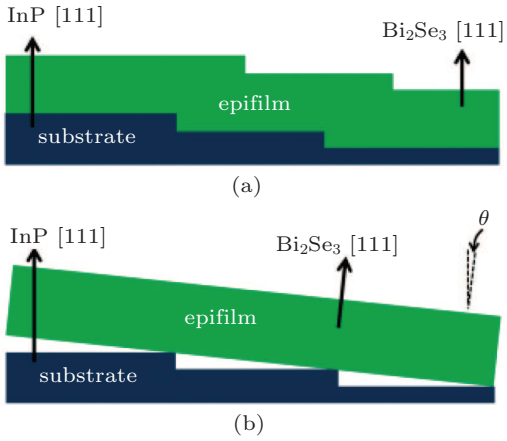


Fig. 6. Schematic illustrations showing (a) the "coherent" epitaxial relation and (b) van der Waals epitaxy on a vicinal substrate such as InP.

4. High-index Bi_2Se_3 epitaxy on InP (001) and GaAs (001) substrates

Until recently, studies of 3D topological insulators like Bi_2Se_3, Bi_2Te_3 or Sb_2Te_3 have focused exclusively on their hexagonal (111) surfaces. This is mainly because of the ease of achieving such surfaces by cleaving bulk crystals or by epitaxial growth of thin films. Surfaces other than the (111) were not available. Attempts to epitaxially grow TI films along other directions than the c axis exist, but were not very successful.[44–47] In these efforts, non-hexagonal substrate surfaces were naturally adopted in order to facilitate high-index Bi_2Se_3 epifilms. Disappointingly, almost all of the past experiments using, e.g., Si (001),[44] Al_2O_3 (110),[45] GaAs(001),[46] and InP (001),[47] resulted in (111) films instead.

Recently, Z. J. Xu *et al.* reported successful growth of a Bi_2Se_3 (221) film on a purposefully treated InP (001) substrate.[48] ARPES measurements of such a sample reveal not only the Dirac cone structure of the surface electrons, but also an elliptical Fermi surface. Correspondingly, magneto-transport studies of such films unveil anisotropic properties.[48,49] Lately, we obtained the same Bi_2Se_3 (221) film, also on a GaAs (001) substrate. Interestingly and importantly, we found that the epifilms are fully strained to fit the lattices of the substrates, even for thick layers.

Figures 7(a) and 7(b) present STM micrographs at different length scales of a surface of epitaxial Bi_2Se_3 (221) on InP (001). Note the striped morphology that is distinctly different from the mounded surfaces of the Bi_2Se_3 (111) films discussed earlier. X-ray diffraction (XRD) and RHEED measurements unambiguously indicate that the epifilm is Bi_2Se_3 (221) with the epitaxial relation of $Bi_2Se_3[\bar{1}\bar{1}0]||InP[\bar{1}\bar{1}0]$, and $Bi_2Se_3[11\bar{4}]||InP[110]$. This is schematically shown in Figs. 8(a) and 8(b).[48]

We remark that such a high-index film is obtainable only on specially roughened substrates containing 3D islands bounded by the {111} facets. The RHEED pattern shows linked spots (Fig. 7(c)). Subsequent Bi_2Se_3 deposition at 443 K smooths the surface and the RHEED pattern becomes streakier (Fig. 7(d)). We believe the Bi_2Se_3 (221) film results via Bi_2Se_3 (111) nucleation on the {111} facets of the substrate, as schematically illustrated in Fig. 8(c). In other words, it is the facetted islands that guide the Bi_2Se_3 (221) film to grow along the surface normal. This conjecture may be supported by an experimental fact that on a smooth InP (001) surface without facetted islands, a Bi_2Se_3 (111) film is obtained instead.[47,48]

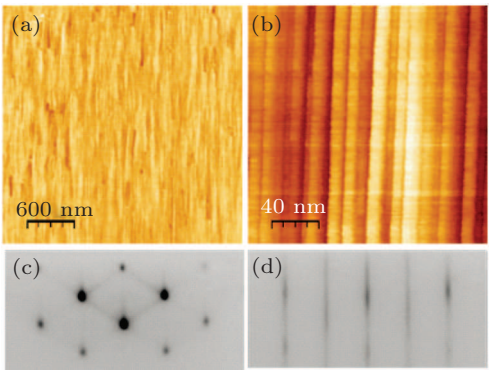


Fig. 7. (a) and (b) STM micrographs of the different length scales of a Bi_2Se_3 (221) film grown on a nominally flat InP (001) substrate. (c) RHEED pattern of the substrate following a thermal treatment prior to Bi_2Se_3 deposition. (d) RHEED pattern after Bi_2Se_3 has been grown. For both RHEED experiments, the electron beam energy was 10 keV, and incident along InP $[1\bar{1}0]$, parallel to the horizontal edges of the STM image. (Panels (a), (c), and (d) are reprinted from *Adv. Mater.***25**, Xue Zhong-Jie *et al.*, "Anisotropic Topological Surface States on High-Index Bi_2Se_3 Films," pp. 1557–1562 (2013), with permission from Wiley-VCH).[48]

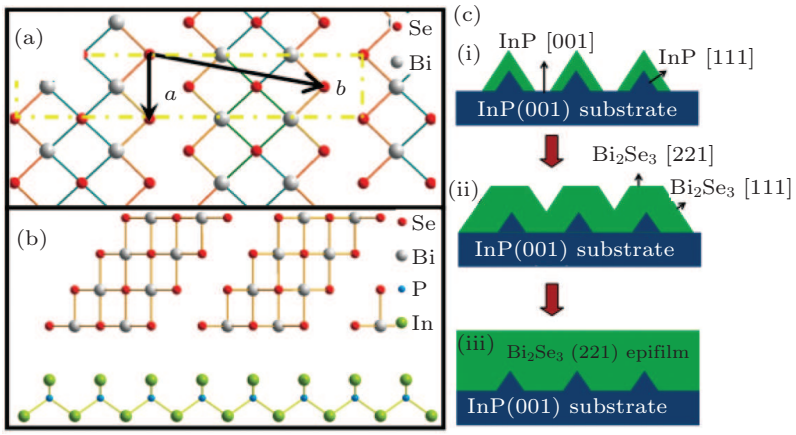


Fig. 8. A model in panel (a) plan-view and panel (b) side-view of an epitaxial Bi_2Se_3 (221) film on an InP (001) substrate (after Ref. [48]). (c) Schematic illustration of Bi_2Se_3 (111) nucleation and growth as guided by the {111} facets of InP, leading to the Bi_2Se_3 (221) epifilm.

Based on the RHEED and LEED measurements, we further find that epitaxial Bi_2Se_3 (221) on either an InP or GaAs substrate is fully strained to fit the lattice of the substrate along the Bi_2Se_3 $[11\bar{4}]$ direction. Such strains are huge, amounting to about 9% stretching on InP. This is possible only because along Bi_2Se_3 $[11\bar{4}]$, there are weakly bonded vdW gaps, as seen from the illustration of Fig. 8(b). Such in-plane stretching does not cause out-of-plane compression, however.[48] The fact that Bi_2Se_3 (221) can be in-plane strained to a large extent by the lattice of the substrate suggests the possibility of probing the effect of such strain on the properties of TIs,[50] a new avenue of research in this important field.

5. Conclusion and perspectives

The layered structure of Bi_2Se_3 makes the compound relatively easy to grow on various substrates by MBE. For the same reason, however, only [111]-oriented films are obtainable on flat substrates, irrespective of the symmetry of their

surface lattices. For growth on hex-symmetrical substrate surfaces, one may still distinguish between the van der Waals type of substrate and those of the non-vdW category, where some differences in growth characteristics are noted. Considering the layered structure of Bi_2Se_3, one would choose a vdW substrate in order to better accommodate the lattice misfit strain. At the heterointerface, the weak vdW bonding between Bi_2Se_3 and the substrate leaves the epifilm unconstrained by the lattices of the substrate, so the epitaxy is incoherent. In other words, the epilayer is fully lattice-relaxed even at the beginning of deposition. It is, however, surprising to observe a slightly stretched lattice of Bi_2Se_3 at the $\sim$ 1 QL coverage. Despite the ease of strain relaxation, experiments have also indicated an advantage of using a lattice-matched substrate for better epitaxial Bi_2Se_3, suggesting a role of misfit strain in the nucleation of Bi_2Se_3, which in turn affects defect formation and lattice alignment. Indeed, rotation and twin domains are common in the epilayers of Bi_2Se_3 grown on vdW substrates. On a non-vdW substrate, a stronger chemical interaction exists between deposited atoms and the substrate, so the lattice of the latter may constrain the lattice of the deposit. First of all, the epilayer is more strained at the beginning stage of deposition. There is also a better alignment of lattices of the deposit to that of the substrate, probably due to a non-negligible effect of the substrate subsurface layers on both the atomic stacking of the deposit and the chemical bonding at steps. Therefore, single-domain Bi_2Se_3 films are obtained on InP(111)A and GaAs(111)A. These results form a basis for future searches for substrates that enable better growth of other layer-structured compounds, including TIs.

Another aspect of TI research is the investigation of surface states on surfaces other than (111). This is encouraged by the recent success in growing Bi_2Se_3 (221) films on facetted InP (001) and GaAs (001) substrates. We find the $\{111\}$ facets on such substrates guide the growth of high-index Bi_2Se_3 (221) films in such a way that a $Bi_2Se_3(111)||InP(111)$ relation is observable. Importantly, for such epitaxial Bi_2Se_3 (221) films, because the vdW gaps are inclined with respect to the surface/interface, they can be tuned by the lattices of the substrate so that the epifilm is fully in-plane strained along one particular crystallographic direction. This leads to a future experimental effort of growing Bi_2Se_3 (221) on some other (001) substrates for different strains, and if available, the strain effect on the TI states can be probed. Furthermore, one may also consider choosing other planes of the substrates, such as the (110) plane of InP and GaAs, for growth of Bi_2Se_3 along other high-index directions.

Acknowledgement

We would like to thank the many people who have contributed to the project over the years, including H. D. Li, Z.Y. Wang, H. T. He, H. C. Liu, J. N. Wang, N. Wang, Q. Li, M. Y. Yao, L. Miao, D. Qian, J. F. Jia, B. Zao and X. Q. Dai — a necessarily incomplete list.

References

[1] Xia Y, Qian D, Hsieh D, Wray L, Pal A, Lin H, Bansil A, Grauer D, Hor Y S, Cava R J and Hasan M Z 2009 *Nat. Phys.* **5** 398
[2] Hsieh D, Xia Y, Qian D, Wray L, Dil J H, Meier F, Osterwalder J, Patthey L, Checkelsky J G, Ong N P, Fedorov A V, Lin H, Bansil A, Grauer D, Hor Y S, Cava R J and Hasan M Z 2009 *Nature* **460** 1101
[3] Checkelsky J G, Hor Y S, Liu M H, Qu D X, Cava R J and Ong N P 2009 *Phys. Rev. Lett.* **103** 246601
[4] Analytis J G, McDonald R D, Riggs S C, Chu J H, Boebinger G S and Fisher I R 2010 *Nat. Phys.* **6** 960
[5] Zhang G H, Qin H J, Teng J, Guo J D, Guo Q L, Dai X, Fang Z and Wu K H 2009 *Appl. Phys. Lett.* **95** 053114
[6] Li H D, Wang Z Y, Kan X, Guo X, He H T, Wang Z, Wang J N, Wong T L, Wang N and Xie M H 2010 *New J. Phys.* **12** 103038
[7] Zhang Y, He K, Chang C Z, Song C L, Wang L L, Chen X, Jia J F, Fang Z, Dai X, Shan W Y, Shen S Q, Niu Q A, Qi X L, Zhang S C, Ma X C and Xue Q K 2010 *Nat. Phys.* **6** 584
[8] Cheng P, Song C L, Zhang T, Zhang Y Y, Wang Y L, Jia J F, Wang J, Wang Y Y, Zhu B F, Chen X, Ma X C, He K, Wang L L, Dai X, Fang Z, Xie X C, Qi X L, Liu C X, Zhang S C and Xue Q K 2010 *Phys. Rev. Lett.* **105** 076801
[9] Richardella A, Zhang D M, Lee J S, Koser A, Rench D W, Yeats A L, Buckley B B, Awschalom D D and Samarth N 2010 *Appl. Phys. Lett.* **97** 262104
[10] Chen J, Qin H J, Yang F, Liu J, Guan T, Qu F M, Zhang G H, Shi J R, Xie X C, Yang C L, Wu K H, Li Y Q and Lu L 2010 *Phys. Rev. Lett.* **105** 176602
[11] He H T, Wang G, Zhang T, Sou I K, Wong G K L, Wang J N, Lu H Z, Shen S Q and Zhang F C 2011 *Phys. Rev. Lett.* **106** 166805
[12] Kou X F, He L, Xiu F X, Lang M R, Liao Z M, Wang Y, Fedorov A V, Yu X X, Tang J S, Huang G, Jiang X W, Zhu J F, Zou J and Wang K L 2011 *Appl. Phys. Lett.* **98** 242102
[13] Li H D, Wang Z Y, Guo X, Wong T L, Wang N and Xie M H 2011 *Appl. Phys. Lett.* **98** 043104
[14] Wang Z Y, Guo X, Li H D, Wong T L, Wang N and Xie M H 2011 *Appl. Phys. Lett.* **99** 023112
[15] Taskin A A, Sasaki S, Segawa K and Ando Y 2012 *Phys. Rev. Lett.* **109** 066803
[16] He L, Xiu F X, Yu X X, Teague M, Jiang W J, Fan Y B, Kou X F, Lang M R, Wang Y, Huang G, Yeh N C and Wang K L 2012 *Nano Lett.* **12** 1486
[17] Tarakina N V, Schreyeck S, Borzenko T, Schumacher C, Karczewski G, Brunner K, Gould C, Buhmann H and Molenkamp L W 2012 *Cryst. Growth Des.* **12** 1913
[18] Zhang L, Hammond R, Dolev M, Liu M, Palevski A and Kapitulnik A 2012 *Appl. Phys. Lett.* **101** 153105
[19] Schreyeck S, Tarakina N V, Karczewski G, Schumacher C, Borzenko T, Brune C, Buhmann H, Gould C, Brunner K and Molenkamp L W 2013 *Appl. Phys. Lett.* **102** 041914
[20] Guo X, Xu Z J, Liu H C, Zhao B, Dai X Q, He H T, Wang J N, Liu H J, Ho W K and Xie M H 2013 *Appl. Phys. Lett.* **102** 151604
[21] Analytis J G, Chu J H, Chen Y L, Corredor F, McDonald R D, Shen Z X and Fisher I R 2010 *Phys. Rev. B* **81** 205407
[22] Wang J, Li H D, Chang C Z, He K, Lee J S, Lu H Z, Sun Y, Ma X C, Samarth N, Shen S Q, Xue Q K, Xie M H and Chan M H W 2012 *Nano Res.* **5** 739
[23] Zhang H J, Liu C X, Qi X L, Dai X, Fang Z and Zhang S C 2009 *Nat. Phys.* **5** 438
[24] Hanaguri T, Igarashi K, Kawamura M, Takagi H and Sasagawa T 2010 *Phys. Rev B* **82** 081305
[25] Koma A 1992 *Surf. Sci.* **267** 29
[26] Koma A 1992 *Thin Solid Films* **216** 72
[27] He L, Xiu F X, Wang Y, Fedorov A V, Huang G, Kou X F, Lang M R, Beyermann W P, Zou J and Wang K L 2011 *J. Appl. Phys.* **109** 103702
[28] Song C L, Wang Y L, Jiang Y P, Zhang Y, Chang C Z, Wang L L, He K, Chen X, Jia J F, Wang Y Y, Fang Z, Dai X, Xie X C, Qi X L, Zhang S C, Xue Q K and Ma X C 2010 *Appl. Phys. Lett.* **97** 143118

[29] Wang Z Y, Li H D, Guo X, Ho W K and Xie M H 2011 *J. Cryst. Growth* **334** 96
[30] Greenberg J 2001 *Thermodynamic Basis of Crystal Growth: P-T-X Phase Equilibrium and Non-stoichiometry* (Berlin: Springer)
[31] Bringans R D and Olmstead M A 1989 *Phys. Rev. B* **39** 12985
[32] Bansal N, Kim Y S, Edrey E, Brahlek M, Horibe Y, Iidad K, Tanimura M, Li G H, Feng T, Lee H D, Gustafsson T, Andrei E and Oh S 2011 *Thin Solid Films* **520** 224
[33] Meyerson B S, Himpsel F J and Uram K J 1990 *Appl. Phys. Lett.* **57** 1034
[34] Xie M H, Seutter S M, Zhu W K, Zheng L X, Wu H S and Tong S Y 1999 *Phys. Rev. Lett.* **82** 2749
[35] Liu F, *private communication*
[36] Vandermerwe J H 1970 *J. Appl. Phys.* **41** 4725
[37] Matthews J W and Blakeslee A E 1974 *J. Cryst. Growth* **27** 118
[38] Burton W K, Cabrera N and FrankF C 1951 *Phil. Trans. R. Soc. A* **243** 299
[39] Liu Y, Weinert M and Li L 2012 *Phys. Rev. Lett.* **108** 115501
[40] Johnson M D, Orme C, Hunt A W, Graff D, Sudijono J, Sander L M and Orr B G 1994 *Phys. Rev. Lett.* **72** 116
[41] Stroscio J A, Pierce D T, Stiles M D, Zangwill A and Sander L M 1995 *Phys. Rev. Lett.* **75** 4246
[42] Ehrlich G and Hudda F 1966 *J. Chem. Phys.* **44** 1039
[43] Schwoebel R L 1969 *J. Appl. Phys.* **40** 614
[44] Ferhat M, Liautard B, Brun G, Tedenac J C, Nouaoura M and Lassabatere L 1996 *J. Cryst. Growth* **167** 122
[45] Tabor P, Keenan C, Urazdhin S and Lederman D 2011 *Appl. Phys. Lett.* **99** 013111
[46] Liu X, Smith D J, Fan J, Zhang Y H, Cao H, Chen Y P, Leiner J, Kirby B J, Dobrowolska M and Furdyna J K 2011 *Appl. Phys. Lett.* **99** 171903
[47] Takagaki Y and Jenichen B 2012 *Semicond. Sci. Technol.* **27** 035015
[48] Xu Z J, Guo X, Yao M Y, He H T, Miao L, Jiao L, Liu H J, Wang J N, Qian D, Jia J F, Ho W K, and Xie M H 2013 *Adv. Mater.* **25** 1557
[49] He H T, Liu H C, Li B K, Wang J N, Guo X, Xu Z J and Xie M H 2013 *unpublished*
[50] Liu W L, Peng X Y, Tang C, Sun L Z, Zhang K W and Zhong J X 2011 *Phys. Rev. B* **84** 245105